 Human Molecular Genetics, 2002, Vol. 11, No. 9 1137–1151

Heat shock protein 27 prevents cellular polyglutamine toxicity and suppresses the increase of reactive oxygen species caused by huntingtin

Andreas Wyttenbach[1], Olivier Sauvageot[2], Jenny Carmichael[1], Chantal Diaz-Latoud[2], Andre-Patrik Arrigo[2] and David C. Rubinsztein[1,*]

[1]Department of Medical Genetics, Cambridge Institute for Medical Research, Wellcome Trust/MRC Building, Addenbrooke's Hospital, Hills Road, Cambridge CB2 2XY, UK and [2]Laboratoire du Stress Oxydant, Chaperons et Apoptose, CNRS-UMR 5534, Universite Claude Bernard Lyon-I, Villeurbanne, France

Received February 13, 2002; Revised and Accepted March 8, 2002

Neuronal loss and intraneuronal protein aggregates are characteristics of Huntington's disease (HD), which is one of 10 known neurodegenerative disorders caused by an expanded polyglutamine [poly(Q)] tract in the disease protein. N-terminal fragments of mutant huntingtin produce intracellular aggregates and cause toxicity. Several studies have shown that chaperones suppress poly(Q) aggregation and toxicity/cell death, but the mechanisms by which they prevent poly(Q)-mediated cell death remain unclear. In the present study, we identified heat shock protein 27 (HSP27) as a suppressor of poly(Q) mediated cell death, using a cellular model of HD. In contrast to HSP40/70 chaperones, we showed that HSP27 suppressed poly(Q) death without suppressing poly(Q) aggregation. We tested the hypotheses that HSP27 may reduce poly(Q)-mediated cell death either by binding cytochrome *c* and inhibiting the mitochondrial death pathway or by protecting against reactive oxygen species (ROS). While poly(Q)-induced cell death was reduced by inhibiting cytochrome *c* (cyt *c*) release from mitochondria, protection by HSP27 was regulated by its phosphorylation status and was independent of its ability to bind to cyt *c*. However, we observed that mutant huntingtin caused increased levels of ROS in neuronal and non-neuronal cells. ROS contributed to cell death because both *N*-acetyl-L-cysteine and glutathione in its reduced form suppressed poly(Q)-mediated cell death. HSP27 decreased ROS in cells expressing mutant huntingtin, suggesting that this chaperone protects cells against oxidative stress. We propose that a poly(Q) mutation can induce ROS that directly contribute to cell death and that HSP27 is an antagonist of this process.

INTRODUCTION

To date, there are at least 10 neurodegenerative diseases caused by abnormally expanded polyglutamine [poly(Q)] tracts in different proteins (1). These diseases are characterized by neuronal loss, which is associated with the appearance of intraneuronal aggregates/inclusions containing the abnormal proteins (or their fragments), including the poly(Q) tract (1). The exact role of these protein aggregates in poly(Q) pathology is controversial (2–4).

The nature of the toxic insult of a poly(Q) mutation and its cell-biological consequences in each disease are unclear, and it is possible that the poly(Q) expansion interferes with basic cellular processes such as transcription, protein degradation and survival/death signalling (5). There is a considerable effort to find molecules that suppress poly(Q) aggregation and cell death/toxicity for therapeutic means (6–8). Heat shock protein (HSP) 40 and HSP70 chaperones have recently been identified as potent modulators of poly(Q) aggregation and/or cell death in in vitro assays (9), in cultured mammalian cells (10–15), in Caenorhabditis elegans and Drosophila models (16,17) and in transgenic mice (18). The HSP40/70 family of chaperones appear to be relevant to poly(Q) disease pathogenesis, since these are associated with the aggregates in cell models, in transgenic mice and in human Huntington's disease (HD) brains (10–15,19).

Different HSPs have recently been shown to directly inhibit several types of cell death pathways induced by a variety of toxic insults in neuronal and non-neuronal cells (20–27). This observation raises the question whether HSPs are able to protect against poly(Q) cell death independently of suppressing poly(Q) aggregation. The small heat shock protein HSP27 has anti-apoptotic properties for which a role in neuronal survival has been suggested (28,29). However, its

*To whom correspondence should be addressed. Tel: + 44 01223 762608; Fax: + 44 01223 331206; Email: dcr1000@cus.cam.ac.uk

role in poly(Q)-mediated cell death/toxicity has not been studied. Elucidation of ways by which HSPs protect cells against poly(Q) mutations might be of relevance for other neurodegenerative conditions where pathology is associated with protein deposition in nerve cells (e.g. α-synuclein in Parkinson's disease, and tau fibrils or Aβ-plaques in Alzheimer's disease).

In the present study, we examined the role of HSP27 in the context of poly(Q) aggregation and cell death, using a cellular model of HD. We found that HSP27 protects neuronal and non-neuronal cells against poly(Q)-mediated cell death without reducing poly(Q)-protein aggregation. We tested the hypotheses that HSP27 may reduce poly(Q)-mediated cell death either by binding cytochrome c (cyt c) and inhibiting the mitochondrial death pathway, or by protecting against reactive oxygen species (ROS). Although we found that poly(Q) cell death was associated with cyt c release and engagement of the mitochondrial death pathway, protection by HSP27 was independent of its ability to bind to cyt c. However, we observed increased levels of ROS in cells expressing expanded compared with wild-type poly(Q) repeats and protection against poly(Q)-mediated cell death/toxicity by antioxidants. The rise of ROS levels induced by the poly(Q) expansion was reduced by HSP27 overexpression. Our findings demonstrate that oxidative stress caused by a poly(Q) expansion contributes to cell death and suggest an important role of HSP27 for preventing neurodegenerative diseases associated with poly(Q) expansions.

RESULTS

Poly(Q) expansion is toxic in the presence and absence of large aggregates, and HSP40/70 chaperones inhibit both aggregation and cell death

We transiently transfected cells with vectors expressing huntingtin exon 1 (httEx1) containing either 23, 25, 53, 74 or 103 glutamines fused to enhanced green fluorescent protein (EGFP) into non-neuronal COS-7 (monkey kidney) or neuronal SK-N-SH (human neuroblastoma) cells. Cells of both cell types expressing httEx1–Q23/25 never produced fluorescent inclusions visible under the microscope (Fig. 1A–C) (data not shown), while cells expressing httEx1–Q53 (data not shown), httEx1–Q74 or Q103 showed the formation of aggregates (Fig. 1D–G) (15). Aggregate formation was time- and poly(Q)-length-dependent in both cell types (15) (data not shown). Aggregates in cells expressing expanded poly(Q)s typically fluoresce much more brightly compared with the diffuse fluorescence in cells expressing either wild-type or mutant huntingtin without aggregates. We monitored cell toxicity by analysing nuclei of transfected (EGFP-expressing) cells for changes associated with cell death, i.e. fragmentation or pyknosis of the nucleus, and we used these changes as a surrogate for cell death and toxicity (see Materials and Methods for details).

Cell death induced by expression of httEx1–Q74 and httEx1–Q103 in SK-N-SH cells was significantly elevated in the absence of visible aggregates, when compared with cells expressing httEx1–Q25 (Fig. 2A). However, httEx1–Q74- and httEx1–Q103-expressing cells with inclusions showed an increase in fragmented/pyknotic nuclei compared with cells expressing the same transgene without visible inclusions (Fig. 2A). We previously reported that cell death induced by expression of httEx1–Q74 in COS-7 cells is not significantly elevated in the absence of visible aggregates, when compared with cells expressing httEx–Q23, but COS-7 cells with inclusions exhibit an increase in cell death (15). These results suggest that the neuroblastoma cell line (SK-N-SH) used in this study was more sensitive to poly(Q)-induced toxicity, compared with a non-neuronal cell line (COS-7). For this reason, in subsequent analyses of poly(Q)-mediated cell death in COS-7 cells, we only considered cells containing inclusions. In experiments with SK-N-SH cells, we analysed all EGFP-positive cells.

The specificity of analysing fragmented/pyknotic nuclei was confirmed, since these changes in nuclear morphology correlated well with propidium iodide (PI) uptake representing dead cells: in live-cell counts, 79.5% ($\pm$1.1%) of httEx1–Q74-expressing COS-7 cells with inclusions showing pyknotic/fragmented nuclei stained positive for PI. In SK-N-SH cells expressing httEx–Q103, 87.5% ($\pm$2.5%) of cells without and 93.9% ($\pm$1.6%) of cells with inclusions showing pyknotic/fragmented nuclei stained positive for PI (data from two independent experiments performed in duplicate). Both COS-7 and SK-N-SH cells expressing httEx1–Q25 with normal nuclear morphology never showed PI uptake. Loss of PI dye exclusion occurs in necrotic and late-stage apoptotic cells, but not in early apoptosis, which probably accounts for the cells with an apoptotic nuclear phenotype with no PI uptake.

In order to test the potential roles of various HSPs in our cell model, we transiently coexpressed these molecules along with our huntingtin exon 1 fragments, using an experimental approach very similar to what has been used previously in analogous studies (10–15). We confirmed previous reports that coexpression of HSP40 (HDJ-1) with httEx1–Q74 inhibited poly(Q) aggregation, with a parallel decrease in cell death in SK-N-SH cells (Fig. 2B, C) (11,13). We also observed these effects by overexpressing HDJ-1 with httEx1–Q103 in SK-N-SH cells and with httEx1–Q53 or –Q74 in COS-7 cells (data not shown). HSP70 reduced both aggregation and cell death in SK-N-SH cells (Fig. 2B, C), which we previously had not observed in COS-7 cells (15). We confirmed overexpression of HDJ-1 and HSP70 above endogeneous levels in cells transfected with HDJ-1 or HSP70, by comparing with mock transfected (empty vector) cells or untransfected cells, using western blotting (Fig. 2D). Figure 1H shows a representative blot of the huntingtin constructs used in most experiments under conditions used in cotransfections.

HSP27 suppresses poly(Q)-mediated cell death without decreasing aggregation

We found that coexpression of hamster HSP27 with httEx1 containing a poly(Q) expansion in COS-7 and SK-N-SH cells did not reduce aggregation formation, but inhibited poly(Q)-mediated cell death significantly (Fig. 3A–D). HSP27 protected SK-N-SH cells against poly(Q)-mediated cell death in the presence and absence of visible aggregates (Fig. 3D). HSP27 overexpression resulted in an increased proportion of cells with aggregates. This phenomenon would occur if aggregates were

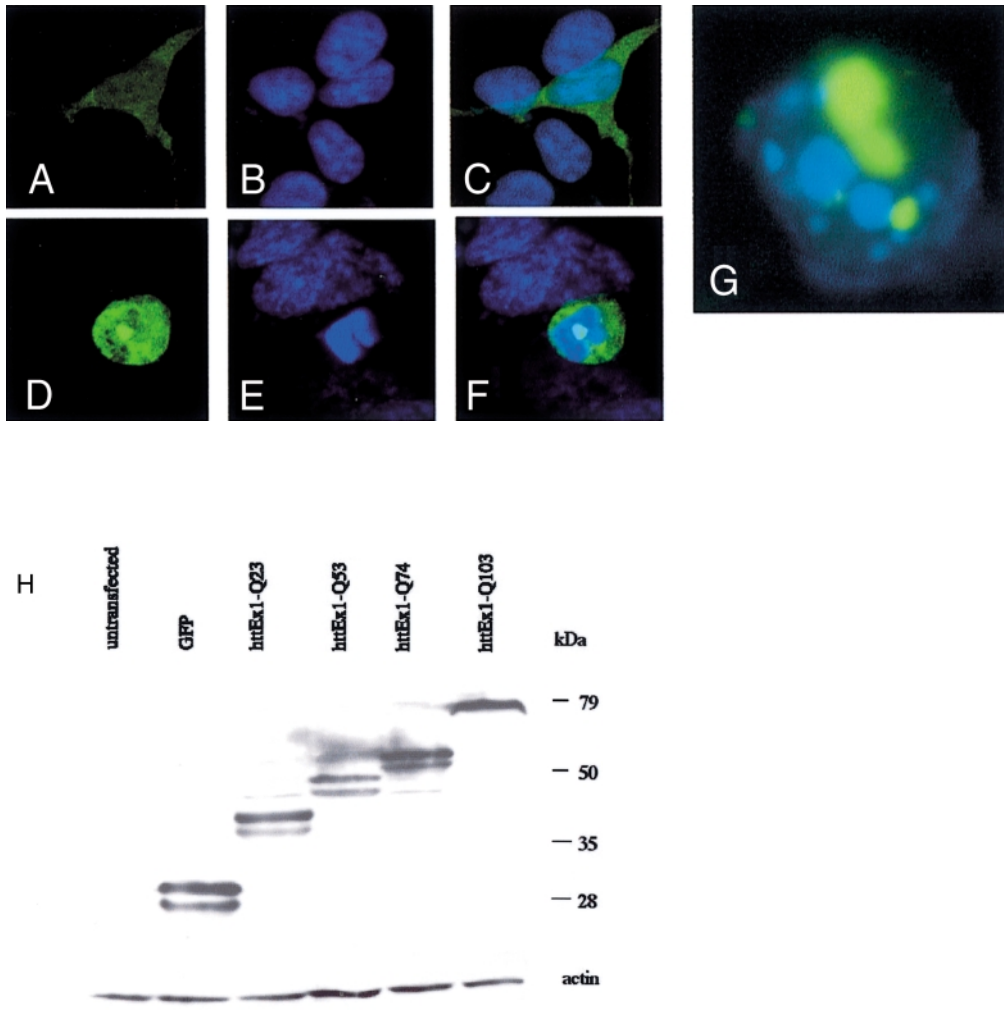

Figure 1. Expression of huntingtin exon 1 (httEx1) fused to EGFP with a polyglutamine expansion forms visible aggregates (A) Diffuse fluorescence of httEx1 with 23 glutamines (green) in SK-N-SH cell. (B) Normal nucleus (DAPI staining, blue). (C) Overlay of (A) and (B). (D) Appearance of poly(Q) aggregate induced by httEx1 with 103 glutamines in SK-N-SH cell. (E) Pyknotic/fragmented nucleus, DAPI staining, (blue) (F) Overlay of (D) and (E). The magnification in (D–F) is slightly larger than in (A–C). Note that the intensity of the fluorescence signal in (D) (EGFP–httEx1–Q103 expression) cannot be compared with the fluorescence signal in (A) (EGFP–httEx1–Q23), since different filter settings needed to be chosen owing to the much higher signal of the aggregate (see text). Cells were transfected, fixed after 48 hours with paraformaldehyde (4%) and analysed using confocal microscopy. We observed similar results in COS-7 cells (not shown). (G) Fragmented nucleus (blue) of a COS-7 cell expressing EGFP–httEx1–Q74 with aggregates (green). (H) Western blot analysis of vectors expressing huntingtin exon 1 with 23, 53, 74 or 103 glutamines fused to EGFP. Expression of EGFP as a non-fusion protein is shown. COS-7 cells were either not transfected or transfected with equal amounts of total DNA (2 μg) comprising EGFP fused to httEx1 and empty vector in a 1 : 3 molar ratio in order to mimic typical conditions used in cotransfection experiments described in Materials and Methods. 48 hours after transfection, whole-cell lysates were run on a SDS–PAGE gel and the same blot was probed with anti-EGFP and anti-actin antibodies (loading control).

protective, an epiphenomenon or deleterious, or if HSP27 modulated cell death but not aggregation – aggregate formation will be more likely in cells that remain attached to a coverslip for longer times owing to the reduced rate of cell death (Fig. 3B). We confirmed overexpression of HSP27 by western blotting (Fig. 2D).

In both cell types, HDJ-1 and HSP70 were sequestered into inclusions (15) (data not shown), but HSP27 was not sequestered (using monoclonal and polyclonal HSP27 antibodies that detected both hamster and human HSP27 on western blots; data not shown). Immunocytochemical analyses suggested no obvious alteration in the predominantly cytoplasmic distribution of either endogenous or exogenously transfected HSP27 in COS-7 and SK-N-SH cells expressing mutant huntingtin fragments, compared with wild-type constructs or untransfected cells (data not shown).

The observation that HSP27 neither reduced poly(Q) aggregation nor showed an altered intracellular distribution, in contrast to HSP40/70 chaperones, suggested to us that its protective mechanism might be distinct from that of HSP40/70. While HSP40/70 chaperones could protect cells against poly(Q)-mediated cell death by binding to expanded poly(Q) proteins and/or reducing poly(Q) aggregation, HSP27 might directly inhibit a cell death pathway engaged by poly(Q) toxicity without inhibiting poly(Q) aggregation. There are no studies on the protective action of small HSPs such as HSP27

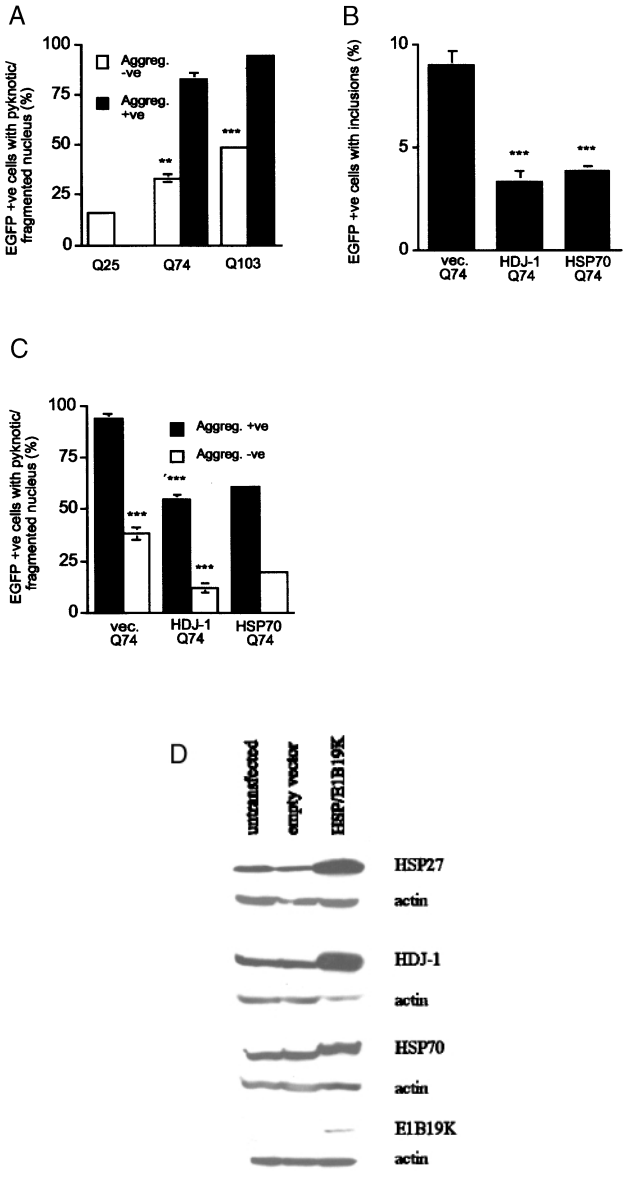

Figure 2. Expression of huntingtin exon 1 (httEx1) with poly(Q) expansions is toxic in the presence and absence of aggregates within SK-N-SH cells. (A) Percentages of SK-N-SH cells transfected with httEx1–Q25, –Q74 or –Q103, showing nuclear abnormalities. Cells with (aggreg. + ve) or without (aggreg. − ve) aggregates were analysed. (B) HDJ-1 and HSP70 coexpression with httQ74 suppress poly(Q) aggregation in SK-N-SH cells (vec., empty vector). (C) Suppression of poly(Q)-mediated cell death by HDJ-1 and HSP70 coexpression in SK-N-SH cells with/without aggregates. For experiments in (A–C), cells were transfected and were fixed after 48 hours, and their nuclei were stained with DAPI. Data from one representative triplicate experiment with standard errors are shown. Statistics from two or three triplicate experiments (see experimental procedures): **, $P < 0.001$; ***, $P < 0.0001$. (D) Western blot analysis of HSP27, HDJ-1, HSP70 and E1B19K overexpression after 48 hours in COS-7 cells. Cells were untransfected or were transfected with empty vector control or the vector expressing the HSP or E1B19K. Note that exogenous HSP70 is tagged (6 × His & Xpress epitope) and hence runs slightly higher on the gel.

on poly(Q)-mediated cell death, despite their potential for preventing poly(Q) pathology. We therefore began to explore the mechanism by which HSP27 is able to reduce poly(Q)-induced cell death without reducing poly(Q) aggregation.

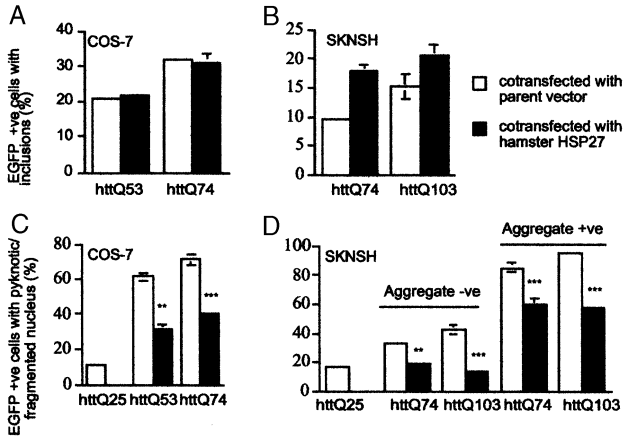

Figure 3. HSP27 does not inhibit huntingtin (httEx1) aggregation, but suppresses its toxicity in the presence and absence of aggregates. (A, B) No suppression of aggregate formation by hamster HSP27 in COS-7 cells (A) and SK-N-SH cells (B). (C, D) Suppression of httEx1-mediated cell death by HSP27 in COS-7 cells (C) and SK-N-SH cells (D) with/without aggregates. For experiments in (A–D), cells were transfected and were fixed after 48 hours, and their nuclei were stained with DAPI. Data from one representative triplicate experiment with standard errors are shown. Statistics from two or three triplicate experiments (see experimental procedures): **, $P < 0.001$; ***, $P < 0.0001$.

HSP27 inhibits the mitochondrial death pathway by binding to and inhibiting apoptosome formation (21). Furthermore, HSP27 is known to protect cells against oxidative stress (30), and this property is dependent on its ability to form large oligomers (30,31). Therefore, we tested the following two hypotheses: (i) poly(Q) toxicity is associated with cyt c release, inhibition of cyt c release blocks poly(Q) death, and HSP27 inhibits mediated cell death through its ability to bind to cyt c; or (ii) poly(Q) expansions directly induce intracellular ROS (oxidative stress), which is suppressed by HSP27.

Inhibition of cyt c release from mitochondria suppresses poly(Q)-mediated cell death

To test if HSP27 inhibited poly(Q)-mediated cell death by interfering at the level of cyt c release, we first had to show that poly(Q)-induced death is indeed associated with cyt c release from mitochondria and that this was of functional significance. Cell death in our model was caspase-dependent and was blocked by the general caspase inhibitor zVAD-fmk in both cell types (15) (data not shown). Overexpression of httEx1 containing poly(Q) expansions in SK-N-SH cells was associated with cyt c release from mitochondria that was not observed in cells overexpressing httEx1-Q25 (Fig. 4). These results were confirmed in COS-7 cells (data not shown), and are consistent with previous observations in HD cell models (32). Similar patterns of cyt c release were seen in staurosporine-treated cells, our positive staining control (data not shown).

Frequently, cyt c release is a late event in apoptosis, where it may be a consequence rather than a cause of cell death (33). It was thus not clear if cyt c release contributed to poly(Q)-induced cell death. We tested if cyt c release is a cause of apoptosis in our model using the anti-apoptotic viral protein

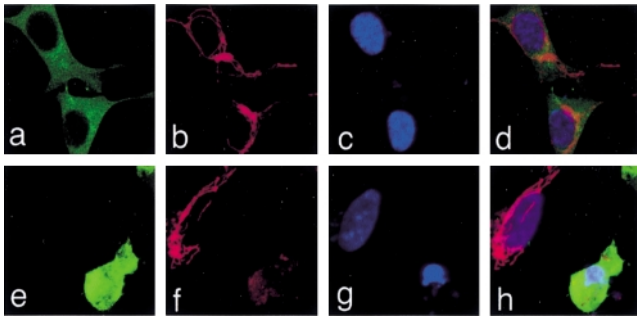

Figure 4. Poly(Q)-mediated cell death is associated with cytochrome c (cyt c) release from mitochondria. (A) SK-N-SH cells (green) expressing httEx1–Q25. (B) cyt c staining is localized to mitochondria (red). (C) Normal nuclei (blue). (D) Overlay of (A–C). (E) SK-N-SH cell expressing httEx1–Q103 (green). (F) Owing to cyt c release from mitochondria of the transfected cell, the staining normally localised to mitochondria is lost and is faintly diffuse throughout the cytoplasm (red). (G) The nucleus is abnormal (condensed, blue). (H) Overlay of (E–G). Note that the magnification for (E–H) is slightly higher and the brightness is enhanced in order to visualize the faint staining of cyt c released from mitochondria. For the experiments in (A–H), cells were transfected and were fixed after 48 hours with paraformaldehyde (4%); immunocytochemistry was performed using a anti-cyt c antibody and analysed using confocal microscopy. We obtained similar results using COS-7 cells. For quantification of cyt c release, see Figure 5.

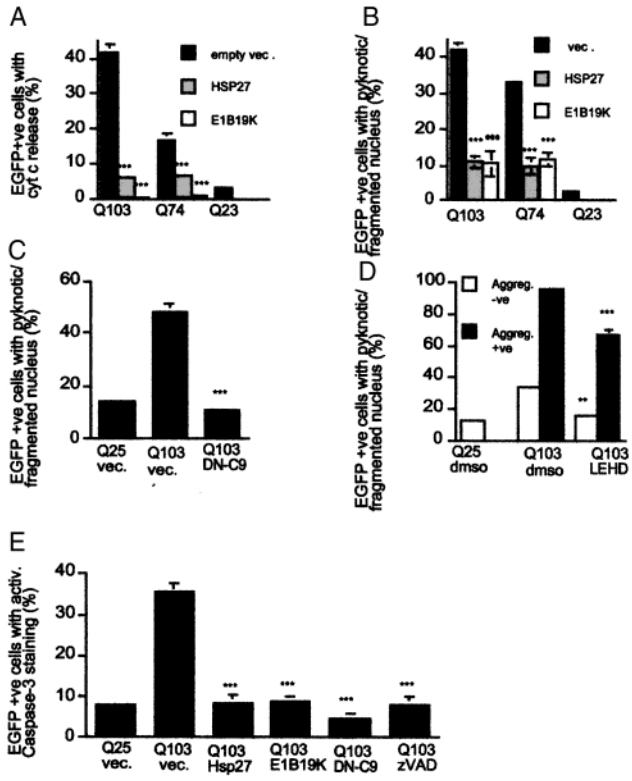

Figure 5. Inhibition of cyt c release reduces poly(Q)-mediated cell death. (A) Percentages of EGFP-positive SK-N-SH cells showing cyt c release when cotransfected with empty vector (vec.), HSP27 or E1B19K; note that HSP27 and E1B19K inhibit cyt c release. (B) Percentages of EGFP-positive SK-N-SH cells showing nuclear abnormalities for the same experiment as in (A). (C) Percentages of EGFP-positive SK-N-SH cells showing nuclear abnormalities when cotransfected with empty vector (vec.) or dominant-negative caspase-9 construct (DN-C9); note the protection against poly(Q)-mediated cell death by DN-C9 coexpression. (D) Poly(Q)-induced cell death is reduced by exposure to the caspase-9-like inhibitor z-LEHD-fmk (100 μM). (E) Caspase-3 activation induced by mutant httEx1 is inhibited by HSP27, E1B19K and dominant negative caspase-9 (DN-C9) coexpression, or exposure to the general caspase inhibitor zVAD-fmk (100 μM). After fixation, immunocytochemistry was performed using an antibody that detects activated caspase-3. The percentage of EGFP-positive cells with positive staining of the active caspase-3 antibody is shown (see Materials and Methods). For experiments in (A–E), cells were transfected and were fixed after 48 hours, and their nuclei were stained with DAPI. Data from one duplicate/triplicate representative experiment with standard errors are shown. Statistics from two or three duplicate/triplicate experiments (see Materials and Methods): **, $P < 0.001$; ***, $P < 0.0001$.

E1B19K, which has previously been shown to block cyt c release (34). E1B19K suppressed both cyt c release and cell death induced by expression of httEx1–Q74 or –Q103 (Fig. 5A, B), without any reduction of aggregate formation in either cell line (data not shown). Expression of E1B19K was confirmed using western blotting (Fig. 2D). Poly(Q)-induced cell death was also reduced by inhibitors of the mitochondrial death pathway acting downstream of cyt c release, such as a dominant-negative caspase-9 construct (Fig. 5C) and a pharmacological inhibitor of caspase-9 (zLEHD-fmk) in SK-N-SH cells (Fig. 5D), without reducing aggregate formation (data not shown). Caspase-9 is thought to be activated after cyt c has been released from mitochondria by the formation of the apoptosome together with Apaf-1 (21). This further demonstrates that the mitochondrial route of cell death was of functional significance in our model. These effects were confirmed in COS-7 cells (data not shown). Since activated caspase-9 is able to cleave and activate caspase-3 (executioner caspase), we examined caspase-3 activation within cells using an antibody that only detects caspase-3 when activated (cleaved fragment of procaspase-3) employing immunocytochemistry. We only scored cells as positive for caspase-3 activation when the staining was clearly above background, and used cells spontaneously undergoing apoptosis in each well or staurosporine-treated cells as a positive control. Caspase-3 activation occurred in SK-N-SH cells overexpressing expanded poly(Q) repeats and was inhibited by coexpression of HSP27, the dominant-negative caspase-9 construct, E1B19K coexpression, or exposure of cells to the general caspase inhibitor zVAD-fmk (Fig. 5E).

If HSP27 primarily prevented cell death by binding to cyt c, one would expect it to reduce cell death without any major effect on cyt c release. However, HSP27 overexpression in cells transfected with httEx1–Q74 or httEx1–Q103 resulted in a major reduction of cyt c release that was of similar magnitude to the HSP27-mediated reduction in cell death (Fig. 5A, B). Furthermore, 100% of cells overexpressing HSP27 and httEx1–Q74 (or –Q103) that showed cyt c release had nuclear abnormalities, similar to what we observed in cells only overexpressing httEx1–Q74 or –Q103 (data not shown). These data are compatible with HSP27 acting upstream of cyt c release.

A cyt c binding-deficient mutant of HSP27 protects against poly(Q)-induced cell death

HSP27 has been shown to bind to cyt c after its release from the mitochondria and thereby inhibit apoptosome formation (21).

To directly exclude the possibility that HSP27 protects against poly(Q)-mediated cell death by binding to cyt c, we coexpressed httEx1–Q74 and httEx1–Q103 in both cell lines with two human HSP27 cyt c binding-deficient mutants, where amino acid C137 was replaced by an alanine (C137A), or where amino acids 51–88 were deleted (Δ51–88) (21). As a control, we used wild-type human HSP27 and a HSP27 mutant construct where amino H131 was replaced by a lysine (H131L), which does not change its ability to bind to cyt c (21). While the C137A mutant lost its protective activity against poly(Q) death, the Δ51–88 HSP27 mutant that is also unable to bind to cyt c still showed a protective effect in both COS-7 and SK-N-SH cells without reducing aggregation (Fig. 6A and B). Overexpression levels of all HSP27 constructs were verified by western blot analysis (Fig. 6C). This finding shows that the capacity of HSP27 to bind to cyt c is not required for its protective function against poly(Q)-mediated cell death.

The phosphorylation status of HSP27 determines its ability to protect against poly(Q)-induced cell death

HSP27 can also protect cells against oxidative stress (30), and this is dependent on its ability to form large oligomers (31). Phosphorylation of HSP27 at three serine residues (S15, S78, S82) or mimicry of phosphorylation by replacing these serines with aspartates dissociates HSP27 complexes to tetramers and reduces its ability to protect against oxidative stress (31). We tested if molecular mimicry mutants of HSP27 phosphorylation also lose the ability to protect against poly(Q)-induced death. We overexpressed three different mutants where one (S15D), two (S78D, S82D) or all three (S15D, S78D, S82D) serine phosphorylation sites were replaced by aspartate, mimicking the phosphorylation state (31). Figure 7A shows that the S15D mutant construct (S1D) retains its protective function compared with wild-type HSP27 when coexpressed with httEx1–Q74 in COS-7 cells or httEx1–Q103 in SK-N-SH cells. However, the triple mutant HSP27-S15, 78,82D (S3D) did not show protection against poly(Q)-induced death in either cell line and the HSP27-S78,82D mutant (S2D) had a intermediate effect (Fig. 7A). Caspase-3 activation could be similarly inhibited by coexpression of the single mutant HSP27-S15D (S1D), but not the triple mutant HSP27-S15, 78, 82D (S3D) (data not shown), using an antibody that detects activated caspase-3 (see above). Expression from constructs of all three HSP27 phosphorylation mutants was confirmed by western blotting (Fig. 6C).

To further investigate the role of HSP27 phosphorylation in poly(Q)-mediated cell death, we exploited the knowledge that phosphorylation of HSP27 is the result of stimulation of the p38 MAP kinase cascade and subsequent activation of MAPKAP kinases 2/3, which directly phosphorylate HSP27 (35,36). We cultured COS-7 and SK-N-SH cells in the presence and absence of SB203580, a highly specific and cell-permeable inhibitor of p38 kinase. We hypothesized that SB203580 would suppress the activation of MAPKAP kinase 2/3 and prevent phosphorylation of endogeneous HSP27 – this could stabilize endogeneous HSP27 in its large oligomeric active form and enhance protection against poly(Q)-induced death. We used SB203580 at concentrations that were previously shown to

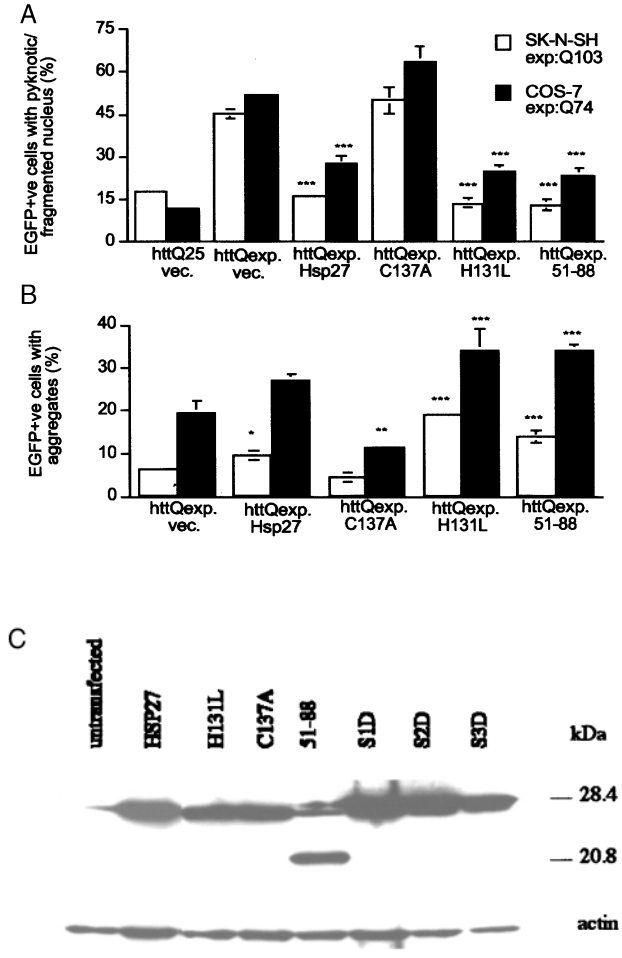

Figure 6. The cyt c binding-deficient HSP27 mutant Δ51–88 protects against poly(Q)-mediated cell death. (A) Percentages of SK-N-SH (open columns) and COS-7 (filled columns) cells with nuclear abnormalities expressing httEx1–Q74 (COS-7) or httEx1–Q103 (SK-N-SH) and cotransfected with either wild-type human HSP27, cyt c binding-deficient mutants (Δ51–88 and C137A), or a mutant that is able to bind to cyt c (H131L). (B) Percentages of EGFP-positive cells containing aggregates for the same experiment as in (A). Cells were transfected and were fixed after 48 hours, and their nuclei were stained with DAPI. Data from one triplicate representative experiment with standard errors are shown. Statistics from two triplicate experiments (see Materials and Methods): *, $P < 0.05$; **, $P < 0.001$; ***, $P < 0.0001$. (C) Western blot analysis showing levels of wild-type and mutant HSP27 overexpression in COS-7 cells 48 hours after transfection (see text). Note that there is background expression of endogenous HSP27 accounting for the 28.4 kDa band in the 51–88 lane. Hsp27, human HSP27 (wild-type); H131L, human HSP27 mutant able to bind to cyt c; C137A, Human HSP27 mutant unable to bind to cyt c; 51–88 (human HSP27 deletion mutant unable to bind to cyt c; S1D, (human HSP27 phosphomimicry mutant of serine 15; S2D, human HSP27 phosphomimicry mutant of serines 15 and 78; S3D, human HSP27 phosphomimicry mutant of serines 15, 78 and 82.

efficiently inhibit p38 MAP kinase (37). At both 1 and 10 μM, SB203580 reduced nuclear abnormalities in SK-N-SH cells induced by httEx1–Q103 (Fig. 7B). While SB203580 at 1 μM also suppressed poly(Q)-mediated cell death in COS-7 cells, a concentration of 10 μM resulted in general cellular toxicity (Fig. 7B and data not shown). Overexpression of a constitutively active MAPKAP kinase 2 construct that phosphorylates HSP27 (38) resulted in increased toxicity in both cell types,

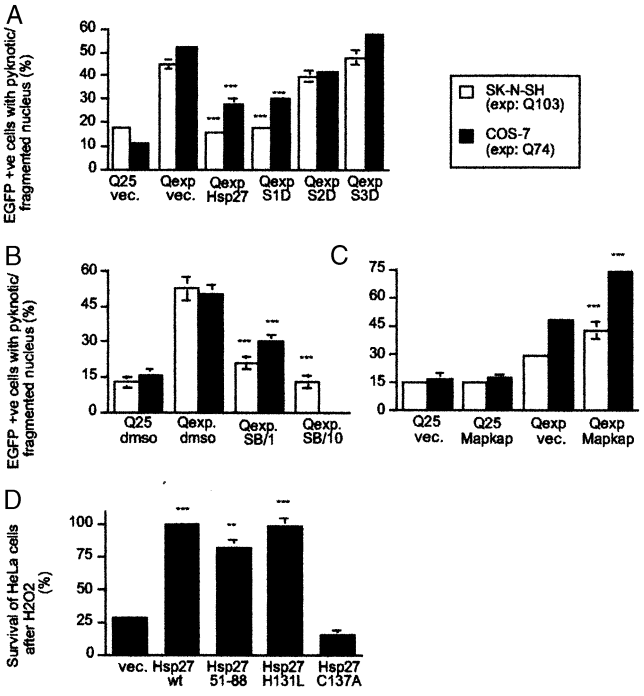

Figure 7. The phosphorylation status of HSP27 determines its protective activity against poly(Q)-mediated cell death. (A) Percentages of SK-N-SH (open columns) and COS-7 (filled columns) cells with nuclear abnormalities expressing httEx1–Q74 (COS-7) or httEx1–Q103 (SK-N-SH) and cotransfected with phosphorylation mutants of HSP27 where serine 15 (S1D), serines 15 and 78 (S2D) or serines 15, 78 and 82 (S3D) were replaced by aspartate. (B) The p38 MAP kinase inhibitor SB203580 protects against poly(Q)-mediated cell death. Cells transfected with mutant httEx1 were grown for 48 hours (SK-N-SH: open columns; COS-7: filled columns) in the presence/absence of SB203580 (SB/1: 1 μM, SB/10: 10 μM) and the percentages of cells with nuclear abnormalities are shown; 10 μM of SB203580 resulted in non-specific toxicity in COS-7 cells (see results). (C) Coexpression of MAPKAP kinase 2 with mutant httEx1 increases its toxicity. SK-N-SH cells (open columns) and COS-7 cells (filled columns) were cotransfected with either empty vector (vec.) or a MAKAP kinase 2-expressing plasmid. For experiments in (A–C), cells were transfected and were fixed after 48 hours, and their nuclei were stained with DAPI. Data from one triplicate representative experiment with standard errors are shown. Statistics from two or three triplicate experiments (see Materials and Methods). (D) HSP27 mutants that protect against poly(Q)-induced death also protect against oxidative stress induced by hydrogen peroxide (H_2O_2). HeLa cells were transfected with the respective plasmids and exposed to 400 μM of H_2O_2 (see Materials and Methods). An unpaired t-test was performed on data from three independent experiments: **, $P < 0.001$; ***, $P < 0.0001$.

further suggesting that endogeneous HSP27 in its unphosphorylated form in both cell types is involved in protection against poly(Q)-induced death (Fig. 7C).

Because the phosphorylation of HSP27 not only reduces its ability to protect against poly(Q)-induced death, but also its ability to protect against cell death due to oxidative stress (30,31), we favoured the hypothesis that this HSP might protect against ROS induced by poly(Q) expansions. Before investigating this hypothesis extensively, we tested if the HSP27-Δ51–88 cyt c binding-deficient and HSP27-H131L mutants that showed protection in our poly(Q) model (Fig. 6A) were also able to protect against ROS toxicity induced by hydrogen peroxide (H_2O_2). Indeed, overexpression of HSP27-Δ51–88 and HSP27-H131L increased survival of HeLa cells exposed to H_2O_2 to a level similar to that obtained by wild-type HSP27 (Fig. 7D). On the other hand, the HSP27-C137A mutant that did not protect against poly(Q)-mediated death (Fig. 6A) was also unable to protect against H_2O_2-induced cell death (Fig. 7D). Both HSP27-Δ51–88 and HSP27-C137A are unable to bind to cyt c and cannot protect cells against etoposide-induced cell death (21). However, despite the failure of HSP27 to bind to cyt c on deletion of amino acids 51–88, this mutation affords protection against H_2O_2-induced death (Fig. 7D), suggesting that protection by HSP27 against oxidative stress is independent of its protective function mediated through cyt c binding.

HSP27 suppresses intracellular ROS induced by poly(Q) expansion

If the protective action of HSP27 against poly(Q)-mediated cell death was indeed due to its anti-oxidant ability, as suggested by our previous experiments, it was possible that a poly(Q) expansion may induce oxidative stress by producing reactive oxygen species (ROS). To test this idea, we transiently overexpressed httEx1 containing 74 glutamines N-terminally fused to a haemagglutinin (HA) tag (HA–httQ74) in SK-N-SH, COS-7 and HeLa cells and used the oxidation-sensitive compound, dichlorofluorescein diacetate (DCFH-DA) to measure intracellular ROS (see Materials and Methods). Since this assay measures green fluorescence, we could not use our EGFP-tagged vectors. We have previously shown that HA–httQ74 induces aggregate formation and increased cell death compared with HA–httQ23, similar to what we observed when overexpressing httEx1 fused to EGFP (see above) (15,39) (data not shown). Forty-eight hours after transfection with these constructs, cells were loaded with DCFH-DA and then in vivo measurements of intracellular ROS were performed during a 1-hour period at 10-minute intervals (see Materials and Methods). HA–httQ74 induced more ROS than HA–httQ23 or empty vector control in HeLa, COS-7 and SK-N-SH cells (30-minute time point, Fig. 8), and we observed similar findings in L929 cells (data not shown). At each time point (4, 10, 20, 30, 40, 50 and 60 minutes), we measured a similar difference in DCFH oxidation for empty vector-, HA–httQ23- and HA–httQ74-transfected cells when compared with the 30-minute time point (data not shown). DCFH fluorescence in cells expressing empty vector, HA–httQ23 and HA–httQ74 rapidly increased and converged to a single point after addition of H_2O_2 (200 μM), showing that there was equal DCFH loading in all cases (positive control; data not shown). We obtained similar transfection efficiencies (see Materials and Methods) and expression levels of the HA–httQ74 and HA–httQ23 transgene for each treatment (data not shown). These results suggested that huntingtin with a poly(Q) expansion induced oxidative stress.

To test if oxidative stress indeed contributed to poly(Q)-mediated cell death, we hypothesized that protection against oxidative stress may ameliorate the cellular phenotype in poly(Q) disease models. N-Acetyl-L-cysteine (NAC), at a concentration shown to have an antioxidant mode of action (1 mM), inhibited poly(Q)-mediated cell death in COS-7 and SK-N-SH cells transfected with either httEx1–Q74 or httEx1–Q103, respectively (Fig. 9). Higher concentrations of NAC

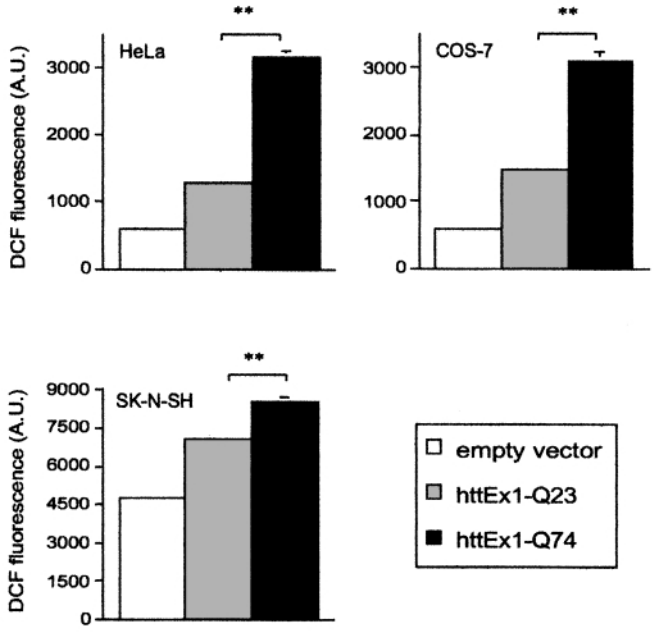

Figure 8. Mutant huntingtin (httEx1) induces increased levels of ROS. Comparison of ROS levels in HeLa, COS-7 or SK-N-SH cells that were transfected with empty vector, HA-tagged httEx1–Q23 or –Q74. Cells were analysed after 48 hours of transfection, with similar transfection efficiencies and expression levels of transgenes in each treatment and cell type (see Materials and Methods). After exposure of cells to DCFH-DA, which is oxidized to fluorescent DCF by intracellular ROS, fluorescence was estimated in vivo at 4, 10, 20, 30, 40, 50 and 60 minutes and expressed in arbitrary units (A.U.). Data for the 30-minute time point from three independent transfection experiments are shown [means with error bars (SD)]. Note that error bars are not visible when SDs are very small. Identical trends to what is shown at 30 minutes were observed at all other time points (data not shown). **, $P < 0.001$; ***, $P < 0.0001$ (unpaired t-test).

(10–50 mM) that were shown to have a survival-promoting effect in PC12 cells deprived of nerve growth factor (NGF) (40) exhibited severe toxicity (data not shown). Exposure of cells to 1 mM of NAC for 48 hours did not significantly reduce aggregation formation in both cell lines (data not shown). Similarly, exposure of cells to the reduced form of glutathione (GSH, 5 mM) inhibited cell death in both cell types (Fig. 9) without reducing aggregation (data not shown). Exposure of SK-N-SH cells to higher concentrations of GSH (50 mM) increased protection (data not shown). These data show that a poly(Q) expansion mutation can induce oxidative stress by increasing intracellular ROS levels and that increased levels of ROS contribute to poly(Q)-mediated cell death.

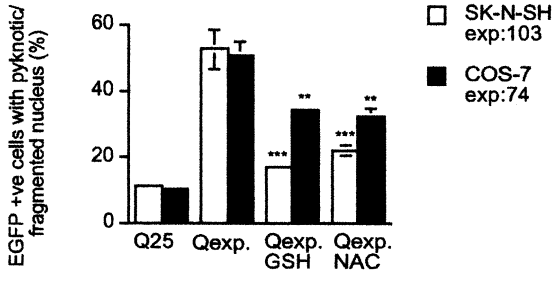

Figure 9. N-Acetyl-L-cysteine (NAC) and glutathione (GSH) protect against poly(Q)-mediated cell death. Cells were grown in the presence/absence of GSH (glutathione ethylester, 5 mM) or NAC (5 mM) after transfection with EGFP–httEx1–Q25/74/103, and cell death was estimated. Data from two independent transfection experiments in triplicate are shown: **, $P < 0.001$; ***, $P < 0.0001$.

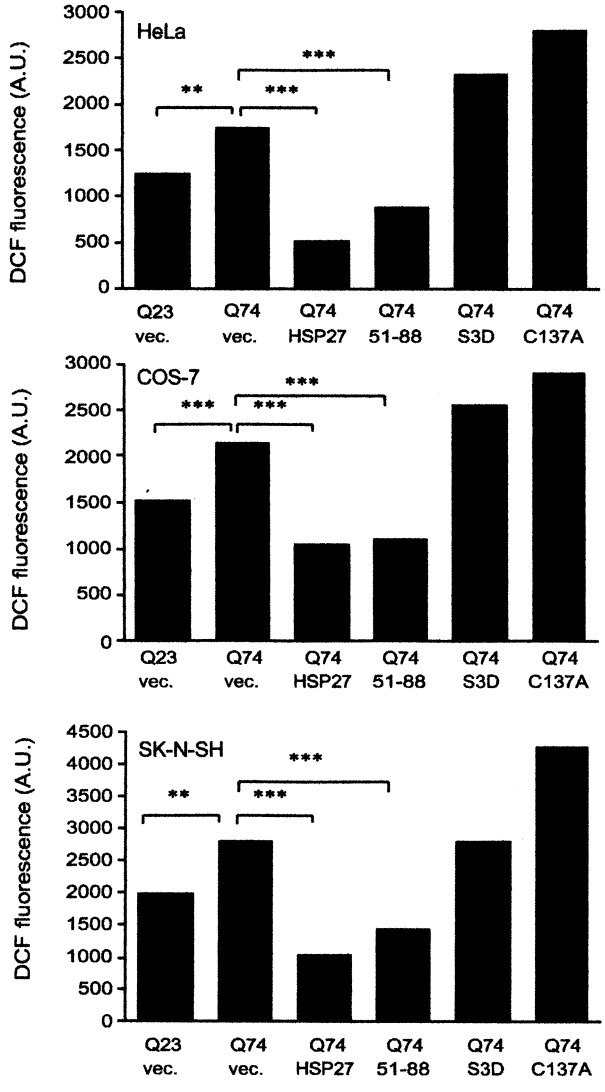

Figure 10. HSP27 reduces increased levels of ROS induced by mutant huntingtin (httEx1). Comparison of ROS levels in HeLa, COS-7 or SK-N-SH cells that were cotransfected with HA-tagged httQ23/74 and empty vector or HSP27/mutants, Note that both wild-type HSP27 and the cyt c binding-deficient mutant Δ51–88 [which also protects against poly(Q)-induced death] reduce ROS, but no reduction was seen with the triple phosphorylation mimicry mutant S3D (S15,78,82D) or the C137A mutant [these mutants do not protect against poly(Q)-mediated cell death]. After exposure of cells to DCFH-DA, which is oxidized to fluorescent DCF by intracellular ROS, fluorescence was estimated in vivo at 4, 10, 20, 30, 40, 50 and 60 minutes and expressed in arbitrary units (A.U.). Data for the 30-minute time point from three independent transfection experiments are shown [means with error bars (SD)]. Note that error bars are not visible when SDs are very small. Identical trends to what is shown at 30 minutes were observed at all other time points (data not shown). **, $P < 0.001$; ***, $P < 0.0001$ (unpaired t-test).

The finding that a poly(Q) mutation in huntingtin caused increased levels of ROS that contributed to cell death prompted us to test if ROS production caused by HA–httQ74 was suppressed by HSP27 and the HSP27-Δ51–88 mutant (previously shown to protect against poly(Q)-induced death, Fig. 6A). Indeed, coexpression of both wild-type HSP27 and the HSP27-Δ51–88 mutant with HA–httQ74 reduced DCF fluorescence in HeLa, COS-7 and SK-N-SH cells (Fig. 10). However, both the HSP27-S3D phosphorylation mimicry mutant (serines 15, 78 and 82 replaced by aspartate) and the C137A mutant were unable to reduce elevated levels of ROS (Fig. 10). These two HSP27 mutants were also ineffective in protecting against poly(Q)-mediated cell death (Fig. 6A). The increased ROS levels in cells expressing HA–httQ74 and HSP27-S15,78,82D or C137A compared with HA–httQ74 and empty vector is possibly a dominant-negative effect: these mutants might form defective 'hybrid-oligomers' with endogeneous HSP27. The differences in DCF fluorescence observed after 30 minutes. (Fig. 10) were confirmed at each time point measured over the 1-hour period (4, 10, 20, 30, 40, 50 and 60 minutes) (data not shown). We observed similar trends in COS-7, SK-N-SH and HeLa cells, and therefore our results are not due to cell-specific phenomena (Fig. 10).

The increased ROS levels associated with HA–httQ74 expression correlated with decreased levels of GSH when compared with cells expressing HA-httQ23 or empty vector in all cell types tested (HeLa, COS-7, SK-N-SH, L929) using the fluorescent probe monochlorobimane (MCB) (Fig. 11A; data not shown). We next investigated if coexpression of wild-type HSP27 or the Δ51–88 mutant with HA–httQ74 were able to restore GSH content. Both wild-type HSP27 and the Δ51–88 mutant (which protected against poly(Q)-induced death and suppressed ROS) increased GSH in HA–httQ74-expressing cells (Fig. 11B). The triple phosphorylation mutant of HSP27 (S3D: S15,78,82D) and HSP27-C137A (which neither protected against poly(Q)-induced death nor inhibited ROS) did not increase intracellular GSH content. These results were consistent across all three cell types tested.

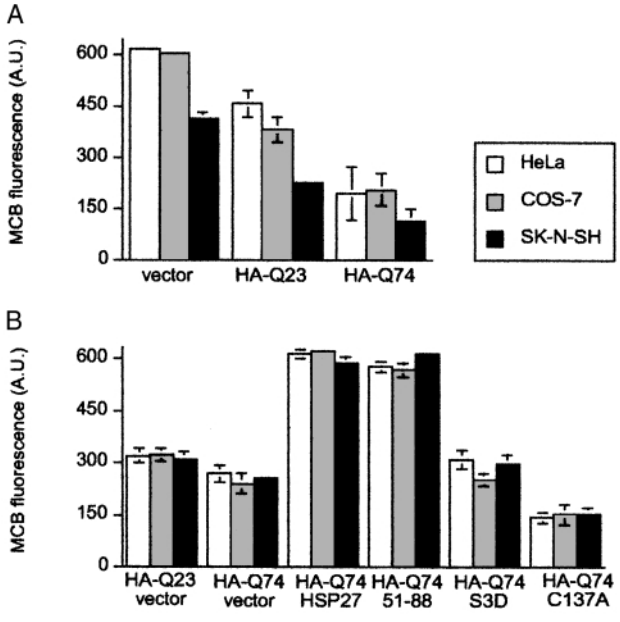

Figure 11. Cells expressing mutant huntingtin (httEx1) have decreased levels of reduced glutathione (GSH), which is increased by coexpression of HSP27. (A) Comparison of cellular content of GSH in HeLa, COS-7 and SK-N-SH cells expressing empty vector or HA-tagged httEx1–Q23 or –Q74; there is a significant reduction of GSH levels in Q74 cells versus Q23 cells in all cell types ($P < 0.05$). (B) Comparison of GSH levels in cells coexpressing HA-tagged httQ74 and empty vector or wild-type HSP27 or mutants. Q74 cells expressing empty vector show a reduction in GSH levels compared with Q23 cells (all cell types; $P < 0.05$). Note that coexpression of wild-type HSP27 and the cyt c binding-deficient mutant Δ51–88 increase intracellular GSH levels in Q74 cells compared with empty vector (all cell types; $P < 0.001$), but not the triple phosphorylation mimicry mutant S3D (S15,78,82D) (all cell types; not significant). There are decreased GSH levels in Q74 cells for the C137A mutant compared with empty vector (all cell types; $P < 0.05$). Also note the inverse relation between ROS and GSH levels (Figs 8 and 10). For all experiments, the total GSH cellular content was determined using monochlorobimane (MCB) (see Materials and Methods). Paired t-tests were performed on data from three independent transfection experiments in (A) and (B) [means with error bars (SD) are presented].

DISCUSSION

Our cellular HD model allowed us to investigate the effects of HSP27, HSP40 (HDJ-1) and HSP70 overexpression on poly(Q) aggregation and cell death. Many mammalian cellular models of poly(Q) disease have shown that overexpression of poly(Q) proteins containing a poly(Q) expansion results in toxicity/cell death, but no clear distinction has been made between cells that contained poly(Q) aggregates or not. We observed that SK-N-SH cells without visible aggregates expressing httEx1 with 74 or 103 glutamines had higher levels of nuclear fragmentation/pyknosis compared with cells expressing wild-type repeat lengths. While our data are consistent with studies in Drosophila and mouse models of poly(Q) disease where exogeneous expression of poly(Q) proteins appeared to be toxic in the absence of detectable aggregates (41,42), we cannot discern if death is caused by 'microaggregates' (oligomers or polymers), as proposed by Conway and colleagues (43) for α-synuclein, or by monomeric httEx1, since we have quantified aggregates microscopically. Cells used in this study that contained large aggregates always showed increased levels of nuclear fragmentation/pyknosis, compared with cells expressing poly(Q) expansions without visible aggregates.

The HSP40/70 family of chaperones appear to be relevant to poly(Q) disease pathogenesis, as these are associated with aggregates in cellular, Drosophila and mouse models of poly(Q) disease (e.g. 10–16,19). Furthermore, some of the HSP40/70 homologues colocalize with ataxin-1 and ataxin-3 aggregates in human brain (10,11). The role of chaperones in poly(Q) diseases as therapeutic agents deserve serious attention, as stressed in the review by Sherman and Goldberg (5), since they prevent aggregation of expanded poly(Q) tracts in recombinant proteins in vitro (9,13) and in several mammalian cell models (10–14, and this study). We showed that HDJ-1 and HSP70 reduced cell death in cells expressing mutant httEx1 without visible aggregates to levels similar to those seen in cells expressing comparable amounts of wild-type httEx1 (Fig. 2). HDJ-1 and HSP70 have been previously shown to be able to suppress poly(Q) aggregation and cell death in parallel

(11–13), but to our knowledge this is the first report showing that these HSPs are protective in cells that do not show visible aggregates. Therefore, some of the protective effects of HSPs may be independent of any effects on poly(Q) aggregation. While we were writing this paper, Zhou et al. (44) indeed reported that suppression of cellular toxicity of huntingtin by HSP40 and HSP70 can be due to inhibition of caspase activation, rather than an effect on aggregation. Therefore, HSP40/70 chaperones may prevent poly(Q)-mediated cell death not only through preventing aggregation, but also by suppressing or delaying caspase activation induced by a poly(Q) insult.

The idea that HSPs can directly rescue cell death in poly(Q) diseases is supported by our novel finding that HSP27 reduced cell death in both COS-7 and SK-N-SH cells, but did not reduce the number of cells with aggregates. HSP27 has also been coexpressed with poly(Q) proteins by Chai et al. (11) and Jana et al. (12), who also observed no reduction of aggregation. We investigated the intracellular distribution of endogeneous and exogeneous HSP27 in poly(Q)-expressing cells using immunocytochemistry. HSP27 staining was mainly found in the cytoplasm and appeared not to be affected by expression of expanded poly(Q), compared with wild-type repeats. However, in contrast to HDJ-1 and HSP70, HSP27 did not redistribute to inclusions, as also observed by Chai et al. (11). Jana and colleagues reported a poly(Q) length-dependent interaction of truncated htt (amino-acids 1–90) with HSP40/70 chaperones (12). Their co-immunoprecipitation experiments showed that an N-terminal segment of htt with an expanded poly(Q) tract bound to HDJ-1 and HSP70, but not to HSP27 (12). The fact that HSP27 is unable to suppress poly(Q) aggregation and appears neither to bind to htt exon1 with a poly(Q) expansion nor redistribute to inclusions strongly suggests that HSP27 protects against poly(Q) toxicity by acting on cell survival/death pathways independent of aggregation suppression.

We tested two likely mechanisms whereby HSP27 could protect against poly(Q)-mediated cell death. First, HSP27 can bind to cyt c, preventing the formation of the apoptosome, thereby inhibiting the mitochondrial cell death pathway (21). Second, HSP27 could protect against oxidative stress (30,31). Prior to testing the first hypothesis, we confirmed previously reported observations that mutant httEx1 was associated with cyt c release (32). The release of cyt c from mitochondria is a universal feature of apoptosis and can either be a primary cause of apoptosis acting as an upstream event or used as an amplification step for a death signal. Frequently, cyt c release is a late event in apoptosis, of which it may be a consequence rather than a cause (33). To assess if cyt c release had any functional role during poly(Q)-induced death, we inhibited cyt c release by E1B19K coexpression and showed that poly(Q)-mediated cell death was indeed suppressed significantly. In addition, inhibition of caspase-9 by coexpression of a dominant-negative caspase-9 construct or a pharmacological caspase-9 inhibitor also reduced cell death. Caspase-9 is thought to be activated after cyt c has been released from mitochondria by the formation of the apoptosome together with Apaf-1 (21). Thus, we have shown that the mitochondrial cell death pathway/cyt c release from mitochondria contributes significantly to poly(Q)-induced death. However, some cells without cyt c release still showed nuclear fragmentation/pyknosis, indicating that poly(Q)-induced cell death may involve cyt c-dependent and cyt c-independent pathways. E1B19K and HSP27 overexpression had similar effects on the reduction of poly(Q)-mediated cell death and on the inhibition of cyt c release. Therefore, it is possible that both molecules inhibit poly(Q)-induced cell death upstream of the mitochondria.

We used two mutants of HSP27 that lost their ability to bind cyt c in order to specifically test if the protective action of HSP27 against poly(Q)-mediated cell death was due to cyt c binding. While the HSP27-C137A mutant lost its protective ability, the deletion mutant HSP27-Δ51–88 still protected against poly(Q)-induced death. This indicates that the protective activity of HSP27 during poly(Q)-induced death did not require binding to cyt c. The differences between the effects of HSP27-C137A and HSP27-Δ51–88 on poly(Q)-induced cell death may be explained by their capacities to protect against oxidative stress – overexpression of HSP27-Δ51–88, but not of HSP27-C137A, reduced cell death provoked by H_2O_2 (Fig. 7D). If HSP27 protected primarily by binding to cyt c, then HSP27-transfected cells would be expected to have similar levels of cyt c release, compared with cells transfected with an empty vector control, and the cells with cyt c release would show less cell death in the presence of HSP27 overexpression, compared with controls. However, in our cell model, HSP27 overexpression resulted in a similar reduction of cell death and cyt c release. Furthermore, in both control cells and HSP27-overexpressing cells, poly(Q) toxicity was associated with cell death in 100% of cells showing cyt c release. Thus, we suspected that HSP27 may act predominantly upstream of cyt c release in our model.

Unphosphorylated HSP27 in its large oligomeric state protects against oxidative stress and this protection is impaired by molecular mimicry of HSP27 phosphorylation that leads to a significant decrease of the oligomeric size of HSP27 (30,31). Therefore, we decided to investigate if the phosphorylation status of HSP27 determined its protective activity against poly(Q)-induced death. We observed that phosphorylation mimicry mutants of HSP27 showed impaired protection against poly(Q)-mediated cell death. Also, the HSP27-Δ51–88 deletion mutant and the HSP27-H131L mutant that protected against poly(Q)-mediated death also protected against oxidative stress induced by H_2O_2 in HeLa cells. Hence, HSP27 mutants/phosphorylation states that protect against oxidative stress are the same as those that protect against poly(Q)-induced death. The importance of the phosphorylation status of HSP27 for protection against poly(Q)-induced death was further supported by our finding that overexpression of constitutively active MAPKAP kinase 2 (which phosphorylates HSP27, preventing its oligomerization) increased poly(Q)-mediated cell death, consistent with the idea that the large oligomeric form of HSP27 is the protective species. Conversely, prevention of endogenous HSP27 phosphorylation by the p38 kinase pathway using SB203580 protected cells against poly(Q)-induced death, although we cannot exclude the possibility that inhibition of the p38 MAP kinase may protect via other mechanisms.

There is in vivo evidence for free-radical damage in an HD mouse (45) and oxidative damage in HD parietal cortex (46), and Li et al. (32,47) showed SOD-2 upregulation in cells

expressing httEx1 with 150 glutamines. Although oxidative stress has been implicated in HD and other late-onset neurodegenerative conditions (48), it is unclear if ROS are a cause or epiphenomenon of pathology in these diseases. Since the same HSP27 mutants/phosphorylation states protected against oxidative stress and poly(Q)-mediated cell death, we began to investigate if a poly(Q) expansion was sufficient to induce elevated ROS and indeed found that HA-tagged exon 1 of huntingtin with 74 glutamines induced more ROS compared with its control (exon 1 with 23 glutamines). Oxidative stress is likely to be relevant to poly(Q)-induced death, since exposure of cells to both NAC and GSH significantly reduced cell death in our model.

The novel observation that expanded poly(Q) huntingtin produced increased levels of cellular ROS gave us the opportunity to directly test if HSP27 protected against poly(Q)-induced death by suppressing ROS. HSP27 and its Δ51–88 deletion mutant both decreased intracellular ROS induced by huntingtin with a poly(Q) expansion. Furthermore, cells expressing huntingtin with a poly(Q) expansion showed lower levels of GSH, which were increased by coexpression of HSP27 and the Δ51–88 deletion mutant. The relatively small but statistically significant reduction in MCB fluorescence in HA-Q74 cells versus HA-Q23 cells in Figure 11B, when compared with Figure 11A, was probably due to decreased amounts of the HD plasmids transfected into the cells in Figure 11B (1.5 μg) versus Figure 11A (3 μg) – in the left-hand six columns of Figure 11B (HA-Q23/vector and HA-Q74/vector), the HD plasmids were cotransfected with empty vectors that served as controls to enable us to test the effects of HSP27 and its mutants on MCB fluorescence. The inverse relation of GSH and ROS would arise if the Q74 cells produced more ROS and therefore induced the oxidation of GSH to GSSG (our method does not detect GSSG but only reduced glutathione). However, we cannot exclude the converse situation that increased ROS levels may be a consequence of the poly(Q) mutation lowering GSH levels. It is possible that overexpression of HSP27 protected against oxidative stress in our model through its glucose-6-phosphate dehydrogenase (G6PD)-dependent ability to increase and maintain levels of reduced GSH (49).

The molecular mechanisms whereby expanded poly(Q)s induce increased ROS levels are unknown. However, it is interesting to note that proteasome inhibition can induce oxidative stress (50,51), and recent data have suggested that proteasome activity may be impaired by poly(Q) expansions (52). Therefore, increased oxidative stress in cells expressing toxic poly(Q)s could be due to inhibition of proteasomal activity. Also, since mitochondria are key players in the production of ROS, they might be important targets of poly(Q) expansion pathology (53). While our data suggest that HSP27 reduces poly(Q)-mediated cell death by modulating the redox state of the cell, we cannot exclude other additional modes of protection. For example, HSP27 may directly inhibit the activation of caspases.

In summary, we have identified HSP27 as a novel poly(Q) disease modifier that, depending of its phosphorylation status, reduces ROS toxicity induced by poly(Q) expansions. A role for HSP27 in neuronal survival has been suggested previously (28,29) and elucidation of the precise mechanisms involved in HSP27-mediated neuroprotection may be of wider relevance to neurodegenerative diseases, since ROS production has been implicated in the pathogenesis of Parkinson's disease, Alzheimer's disease, amyotrophic lateral sclerosis and progressive supranuclear palsy (54).

MATERIALS AND METHODS

Plasmids, transient cotransfection and cell culture

In cotransfection experiments, we used htt exon 1 (httEx1) fused to EGFP containing 23, 53 or 74 glutamines [poly(Q)s at C terminus, EGFP-C1] called httEx1–Q23, 53 or 74, as described previously (15). We used constructs expressing httEx1 fused to EGFP containing 25 or 103 glutamines [poly(Q)s at N terminus, EGFP-N1] (from A. Tobin and G. Lawless, University of California, Los Angeles), human HDJ-1 (HSP40) (from H. Paulson, University of Iowa), human HSP70 (10), hamster HSP27 (from D. Latchman, University College London), human HSP27 constructs and cyt c-binding mutants (described and tested in 21), dominant-negative caspase-9 (C287A) (from E.S. Alnemri, CAR, Philadelphia) (55), constitutively active MAPKAP kinase 2 (3 × Asp) (from S. Hooper, Chester Beatty Laboratories, London) (38) and E1B19K (from A.M. Tolkovsky, Department of Biochemistry, University of Cambridge). Overexpression of all the relevant proteins was verified by western blotting. As an empty vector control, we used matching vectors without an insert (pFLAG-CMV2, Sigma; pcDNA3.1, Invitrogen). The preparation of plasmids used for related experiments (e.g. HSP27 series) was performed at the same time with the same endotoxin-free kit (Qiagen). The concentrations of such related maxipreparations were determined using a spectrophotometer and agarose gels at the same time in order to maximize consistency between plasmid batches.

African green monkey kidney (COS-7) and human neuroblastoma (SK-N-SH) cells were cultured, seeded and transfected as described previously (15). We used a 3 : 1 or 5 : 1 ratio of test construct to httEx1 poly(Q) construct DNA, to ensure that all cells expressing poly(Q) constructs also expressed the appropriate test construct. At 48 hours after transfection, cells on coverslips were fixed with 4% paraformaldehyde in 1 × PBS at room temperature for 20 minutes and mounted in antifadent supplemented with 4′,6-diamidino-2-phenylindole (DAPI) (3 μg/ml) to allow visualization of nuclear morphology.

Estimation of poly(Q) aggregation and cell death/survival

Cells were counted as aggregate-positive if one or several aggregates were visible within a cell. We counted 300–500 EGFP-positive cells in multiple random visual fields per slide, and the figures show a percentage from one representative triplicate experiment, with P-values being derived from odds ratios of pooled estimates from two or three independent triplicate experiments (see Statistical analysis). Cell death/toxicity was monitored by scoring the proportion of transfected cells (EGFP-expressing cells) with apoptotic nuclear morphology – fragmented or pyknotic nuclei. The latter are typically condensed to a diameter of less than 50% of the size of a

normal nucleus and show more intense DAPI uptake compared with normal nuclei. Such abnormal nuclear morphology was largely rescued in cells treated with pan-caspase inhibitors, demonstrating that it is not a non-specific phenomenon. To confirm that cells with pyknosis or fragmentation of the nucleus were indeed dead cells, we performed live cell analysis and determined the percentage of inclusion-containing COS-7 cells expressing httEx1–Q74 and SK-N-SH cells expressing httEx1–Q103 showing nuclear fragmentation or pyknosis and simultaneous loss of propidium iodide (PI) exclusion. Cells were transfected and analysed 48 hours thereafter using PI (5 μg/ml) and Hoechst 33342 (5 μg/ml) staining (5–10 minutes, exposure). Cells expressing httEx1–Q25 with normal nuclear morphology never stained positive for PI, while there was a strong correlation between cells expressing toxic poly(Q)s with nuclear pyknosis or fragmentation and PI uptake (see Results).

All coverslips were scored with the observer blind to the identity of the coverslip, and we counted 100–300 EGFP-positive cells per coverslip. For COS-7 cells, we restricted cell death analysis to cells with aggregates, since COS-7 cells without aggregates do not have increased levels of cell death compared with wild-type httEx1 constructs (15). For SK-N-SH cells, we analysed cells with and without aggregates (EGFP-positive). We used an antibody recognizing activated caspase-3 as a second readout for poly(Q)-mediated cell death in important experiments (see Immunocytochemistry). Cells with fragmented or pyknotic nuclear morphology stained positive for activated caspase-3. Cells with activated caspase-3 staining showed a clearly stronger signal compared with background. As a positive control for caspase-3 activation, we exposed cells to staurosporine. Cells were analysed using a conventional fluorescent microscope. Pictures were taken on a confocal microscope (Leica).

To estimate survival of cells exposed to H_2O_2, control as well as transiently transfected HeLa cells were plated in 96-well tissue culture plates (Nunc, Rockskilde, Denmark) at a density of 7.5×10^4 cells per well, grown for 24 hours, after which 400 μM H_2O_2 was added. Cells were incubated for further 24 hours before analysis. Subsequently, supernatants were discarded and the remaining viable cells were stained with 0.5% crystal violet in 50% methanol for 15 minutes Microtiter plates were rinsed and dried. A medium containing 0.1 M sodium citrate pH 5.4 and 20% methanol was then added to solubilize the stained cells. The absorbance of each well was read after 30 minutes at 570 nm with an MR5000 micro-ELISA reader (Dynatech Laboratories, Chantilly, VA). The percent of cell survival was defined as the relative absorbance of treated versus untreated cells.

Caspase inhibition, GSH, NAC and SB203580 experiments

zVAD-fmk (general caspase inhibitor) and zLEHD-fmk (caspase-9-like inhibitor) (Calbiochem) were used at a final concentration of 100 μM. DMSO served as the solvent control. Glutathione-ethylester (GSH) (Sigma, Dorset, UK) was freshly dissolved in water each time before addition. Cells were exposed to GSH (5 mM) for 12 hours prior to transfection and then GSH was replaced every 12 hours. N-Acetyl-L-cysteine (NAC, 1 mM) (Sigma) was dissolved in culture medium (DMSO), the pH adjusted to 7.4, and was added as described for GSH. SB203580 (Promega) was dissolved in DMSO, added immediately after transfection and replaced every 12 hours.

Immunocytochemistry and western blotting

For HSP colocalization studies, cells were grown on coverslips and after the experimental procedure, cells were either fixed with ice-cold methanol (10 minutes) or 4% paraformaldehyde (20 minutes) at room temperature (RT), washed twice and permeabilized (0.2% Triton X-100 in 1 × PBS) for 15 minutes at RT. After three wash steps with 1 × PBS, cells were incubated in blocking buffer (5% fetal bovine or rat serum) for 30 minutes and exposed to primary antibody for 1–2 hours at RT or overnight at 4°C. Antibodies were rabbit anti-HDJ-1 polyclonal/1 : 1000 (SPA-400, Stressgene, Victoria, CA), rabbit anti-HSP25 polyclonal/1 : 500 (Stressgene), mouse anti-HSP27 monoclonal/1 : 400 (Neomarker), mouse anti-HSP70 monoclonal/1 : 200 (SPA-810, Stressgene), rat anti-HSC70 monoclonal/1 : 400 (Stressgene), mouse anti-cytochrome c monoclonal/1 : 500 (Pharmingen), mouse anti-HA monoclonal/1 : 1000 or rabbit anti-active caspase-3 polyclonal/1 : 250 (Promega). After exposure to the primary antibody, cells were exposed for 30 minutes to blocking buffer and incubated in either goat anti-mouse IgG or goat anti-rabbit IgG conjugated to Texas Red (Molecular Probes) for 2 hours in the dark at RT (1 : 800), dried and mounted in antifadent (Citifluor).

For western blotting, cell pellets were lysed in 1% Triton X-100, 150 mM NaCl, 25 mM Tris–HCl and 0.4% SDS for 30 minutes on ice, and high-speed centrifuged for 20 minutes, and the supernatants were subjected to SDS–PAGE (12%). Primary antibodies were mouse anti-GFP monoclonal (1 : 1000, Clontech), rabbit anti-HDJ-1 polyclonal/1 : 2000 (SPA-400, Stressgene, Victoria, CA), rabbit anti-HSP25 polyclonal/1 : 1000 (Stressgene), mouse anti-HSP27 monoclonal/1 : 1000 (Neomarker), rat anti-E1B19K (gift from A.M. Tolkovsky, Cambridge, UK), mouse anti-HA monoclonal (1 : 1000) and rabbit anti-actin polyclonal (1 : 2500, Sigma). Blots were probed with peroxidase-labeled anti-mouse or anti-rabbit antibodies at 1 : 2500 (Amersham). Bands were visualized with the ECL detection reagent (Amersham). Protein loading was controlled by probing for actin on the same membrane.

Estimation of ROS production and intracellular glutathione

Transient transfection was performed in exponentially growing HeLa, COS-7 and SK-N-SH cells, plated 1 day before transfection in 60 mm dishes. For single-transfection experiments (Figs 8 and 11A), cells were transfected with a mixture of 3 μg of DNA plus 20 μl of Lipofectamine (Gibco, BRL, UK) which were preincubated for 45 minutes and then added to the cells. After 3 hours, the Optimum DNA mixture was replaced with complete growth medium, and cells were analysed for ROS 48 hours later. The HA–httQ23/Q74 vectors have been described previously (39). For double-transfection experiments (Figs 10 and 11B) (HSP27 mutants and HA–httQ23/Q72), we used identical amounts of each vector (1.5 μg DNA). The transfection efficiency (50–80%, depending on the cell line) was compared in parallel experiments using pEGFP (Clontech, Palo Alto, CA) and analysed using fluorescence microscopy to

ensure that similar numbers of cells of each cell type were transfected (data not shown). In vivo measurement of intracellular ROS was performed as previously described (56). Cell types were plated at a density of 7.5×10^4 (HeLa), 6×10^4 (COS-7) or 8×10^4 (SKNSH) per well in a 96-well tissue culture plate. Cells, kept at 37°C, were washed three times with PBS and then with PBS containing dichlorofluorescein diacetate (DCFH-DA) (5 μg/μl) (Molecular Probes–Interchim, Montluçon, France). DCFH-DA is oxidized to fluorescent DCF by different intracellular ROS, particularly those of peroxide origin. Plates were read in a 1420 multilabel counter plate reader (Victor Wallac, Finland) during a 1-hour period (4, 10, 20, 30, 40, 50 and 60 minutes) with an excitation wavelength of 485 nm and an emission wavelength of 530 nm.

Total GSH (reduced form of glutathione) cellular content was determined using the monochlorobimane (MCB) fluorescent probe (56,57). Cells were plated as described above and incubated for 5 minutes with 40 μM MCB in the growth medium before measurement. Fluorescence at 425 nm was analysed in response to an excitation at 395 nm in a 1420 multilabel counter plate reader (Victor Wallac, Finland). To compare transgene expression levels of HA–httQ23 and HA–httQ74 cells in ROS/GSH experiments, cells were lysed in a SDS sample buffer containing 5 M guanidinium chloride (final concentration), vortexed for 3 minutes at room temperature and boiled for 5 minutes before being analysed by SDS–PAGE and immunoblotting as described by Mehlen et al. (56).

Statistical analysis

As a measure of inclusion formation, we considered the proportion of htt exon 1-expressing cells with one or more inclusions. Statistical significance was obtained of pooled estimates of multiple experiments, and expressed as odds ratios (OR) with 95% confidence intervals. ORs compare the proportions of EGFP-expressing cells with or without inclusions when cotransfected with an HSP with the proportions observed when cotransfected with control vectors (same for nuclear abnormalities). ORs were considered to be the most appropriate summary statistics, because the percentage of cells with inclusions or nuclear abnormalities under specified conditions varied between experiments on different days, whereas the relative change in the proportion of cells with inclusions or nuclear abnormalities induced by overexpression of an HSP is expected to be more constant. ORs and P-values were determined by unconditional logistical regression analysis by using the general loglinear option of SPSS 9.1 software (SPSS, Chicago). The P-values presented in each figure were calculated from at least two or three independent experiments performed in triplicate unless stated otherwise. Graphs show the means of one representative experiment performed in triplicate with standard errors, and values are given as a percentage. For some experiments, we performed paired t-tests using the software Statview (V4.5).

ACKNOWLEDGEMENTS

We thank A.M. Tolkovsky for suggesting the use of E1B19K and providing the plasmid and antibody, for stimulating discussions and for a critical review of the manuscript. We are grateful to D. Latchman (Institute of Child Health, London, UK) for the hamster HSP27 construct, S. Hooper (Chester Beatty Laboratories, London, UK) for the MAPKAP kinase 2 construct, M. Gaestel (Martin-Luther University, Halle, Germany) for the HSP27 phosphorylation mimicry vectors, G. Lawless and A. Tobin (University of California, Los Angeles, USA) for EGFP-httQ25/103 vectors and E.S. Alnemri for the dominant caspase-9 plasmid. We thank D. Guillet for excellent technical assistance. We are grateful to the Hereditary Disease Foundation (A.W., D.C.R.), Merck Sharp and Dohme (A.W.), Action Research (J.C.), the Association pour la Recherche sur le Cancer and the Région Rhône-Alpes (Grant No. 5204 to A.P.A.) for financial support. J.C. is grateful for a Sackler studentship. O.S. was supported by a predoctoral fellowship from the Centre regional des Oeuvres Universitaires et Sociales of Lyon. A.W. is a MSD postdoctoral fellow. D.C.R. is grateful for Glaxo Wellcome and Wellcome Trust Senior Clinical Research Fellowships.

REFERENCES

1. Ross, C.A. (1997) Intranuclear neuronal inclusions: a common pathogenic mechanism for glutamine-repeat neurodegenerative diseases? Neuron, 19, 1147–1150.
2. Carmichael, J., Chatellier, J., Woolfson, A., Milstein, C., Fersht, A.R. and Rubinsztein, D.C. (2000) Bacterial and yeast chaperones reduce both aggregate formation and cell death in mammalian cell models of Huntington's disease. Proc. Natl Acad. Sci. USA, 97, 9701–9705.
3. Perutz, M.F. (1999) Glutamine repeats and neurodegenerative diseases: molecular aspects. Trends Biochem. Sci., 24, 58–63.
4. Saudou, F., Finkbeiner, S., Devys, D. and Greenberg, M.E. (1998) Huntingtin acts in the nucleus to induce apoptosis but death does not correlate with the formation of intranuclear inclusions. Cell, 95, 55–66.
5. Sherman, M.Y. and Goldberg, A.L. (2001) Cellular defenses against unfolded proteins: a cell biologist thinks about neurodegenerative diseases. Neuron, 29, 15–32.
6. Heiser, V., Scherzinger, E., Boeddrich, A., Nordhoff, E., Lurz, R., Schugardt, N., Lehrach, H. and Wanker, E.E. (2000) Inhibition of huntingtin fibrillogenesis by specific antibodies and small molecules: implications for Huntington's disease therapy. Proc. Natl Acad. Sci. USA., 97, 6739–44.
7. Kazemi-Esfarjani, P. and Benzer, S. (2000) Genetic suppression of polyglutamine toxicity in Drosophila. Science, 287, 1837–1840.
8. Nagai, Y., Tucker, T., Ren, H., Kenan, D.J., Henderson, B.S., Keene, J.D., Strittmatter, W.J. and Burke, J.R. (2000) Inhibition of polyglutamine protein aggregation and cell death by novel peptides identified by phage display screening. J. Biol. Chem., 275, 10437–10442.
9. Muchowski, P.J., Schaffar, G., Sittler, A., Wanker, E.E., Hayer-Hartl, M.K. and Hartl, F.U. (2000) Hsp70 and hsp40 chaperones can inhibit self-assembly of polyglutamine proteins into amyloid-like fibrils. Proc. Natl Acad. Sci. USA, 97, 7841–7846.
10. Cummings, C.J., Mancini, M.A., Antalffy, B., DeFranco, D.B., Orr, H.T. and Zoghbi, H.Y. (1998) Chaperone suppression of aggregation and altered subcellular proteasome localization imply protein misfolding in SCA1. Nature Genet., 19, 148–154.
11. Chai, Y., Koppenhafer, S.L., Bonini, N.M. and Paulson, H.L. (1999) Analysis of the role of heat shock protein (Hsp) molecular chaperones in polyglutamine disease. J. Neurosci., 19, 10338–10347.
12. Jana, N.R., Tanaka, M., Wang, G.H. and Nukina, N. (2000) Polyglutamine length-dependent interaction of hsp40 and hsp70 family chaperones with truncated N-terminal huntingtin: their role in suppression of aggregation and cellular toxicity. Hum. Mol. Genet. 9, 2009–2018.
13. Kobayashi, Y., Kume, A., Li, M., Doyu, M., Hata, M., Ohtsuka, K. and Sobue, G. (2000) Chaperones Hsp70 and Hsp40 suppress aggregate formation and apoptosis in cultured neuronal cells expressing truncated androgen receptor protein with expanded polyglutamine tract. J. Biol. Chem. 275, 8772–8778.

14. Stenoien, D.L., Cummings, C.J., Adams, H.P., Mancini, M.G., Patel, K., DeMartino, G.N., Marcelli, M., Weige,l N.L. and Mancini, M.A. (1999) Polyglutamine-expanded androgen receptors form aggregates that sequester heat shock proteins, proteasome components and SRC-1, and are suppressed by the HDJ-2 chaperone. Hum. Mol. Genet., 8, 731–741.
15. Wyttenbach, A., Carmichael, J., Swartz, J., Furlong, R.A., Narain, Y., Rankin, J. and Rubinsztein, D.C. (2000) Effects of heat shock, heat shock protein 40 (HDJ-2), and proteasome inhibition on protein aggregation in cellular models of Huntington's disease. Proc. Natl Acad. Sci. USA, 97, 2898–2903.
16. Warrick, J.M., Chan, H.Y., Gray-Board, G.L., Chai, Y., Paulson, H.L. and Bonini, N.M. (1999) Suppression of polyglutamine-mediated neurodegeneration in Drosophila by the molecular chaperone HSP70. Nature Genet., 23, 425–428.
17. Satyal, S.H., Schmidt, E., Kitagawa, K., Sondheimer, N., Lindquist, S., Kramer, J.M. and Morimoto, R.I. (2000) Polyglutamine aggregates alter protein folding homeostasis in Caenorhabditis elegans. Proc. Natl Acad. Sci. USA, 97, 5750–5755.
18. Cummings, C.J., Sun, Y., Opal, P., Antalffy, B., Mestril, R., Orr, H.T., Dillmann, W.H. and Zoghbi, H.Y. (2001) Over-expression of inducible HSP70 chaperone suppresses neuropathology and improves motor function in SCA1 mice. Hum. Mol. Genet., 10, 1511–1518.
19. Wyttenbach, A., Swartz, J., Kita, H., Thykjaer, T., Carmichael, J., Bradley, J., Brown, R., Maxwell, M., Schapira, A., Orntoft, T.F. et al. (2001) Polyglutamine expansions cause decreased CRE-mediated transcription and early gene expression changes prior to cell death in an inducible cell model of Huntington's disease. Hum. Mol. Genet., 10, 1829–1845.
20. Beresford, P.J., Jaju, M., Fiedman, R.S., Yoon, M.J. and Lieberman, J. (1998) A role for heat shock protein 27 in CTL-mediated cell death. J. Immunol., 161, 161–167.
21. Bruey, J.M., Ducasse, C., Bonniaud, P., Ravagnan, L., Susin, S.A., Diaz-Latoud, C., Gurbuxani, S., Arrigo, A.P., Kroemer, G., Solary, E. and Garrido, C. (2000) Hsp27 negatively regulates cell death by interacting with cytochrome c. Nature Cell Biol., 2, 645–652.
22. Saleh, A., Srinivasula, S.M., Balkir, L., Robbins, P.D. and Alnemri, E.S. (2000) Negative regulation of the Apaf-1 apoptosome by Hsp70. Nature Cell Biol., 2, 476–483.
23. Beere, H.M., Wolf, B.B., Cain, K., Mosser, D.D., Mahboubi, A., Kuwana, T., Tailor, P., Morimoto, R.I., Cohen, G.M. and Green, D.R. (2000) Heat-shock protein 70 inhibits apoptosis by preventing recruitment of procaspase-9 to the Apaf-1 apoptosome. Nature Cell Biol., 2, 469–475.
24. Pandey, P., Farber, R., Nakazawa, A., Kumar, S., Bharti, A., Nalin, C., Weichselbaum, R., Kufe, D. and Kharbanda, S. (2000) Hsp27 functions as a negative regulator of cytochrome c-dependent activation of procaspase-3. Oncogene, 19, 1975–1981.
25. Gabai, V.L., Yaglom, J.A., Volloch, V., Meriin, A.B., Force, T., Koutroumanis, M., Massie, B., Mosser, D.D. and Sherman, M.Y. (2000) Hsp72-mediated suppression of c-Jun N-terminal kinase is implicated in development of tolerance to caspase-independent cell death. Mol. Cell. Biol., 20, 6826–6836.
26. Tezel, G. and Wax, M.B. (2000) The mechanisms of hsp27 antibody-mediated apoptosis in retinal neuronal cells. J. Neurosci., 20, 3552–3562.
27. Charette, S.J., Lavoie, J.N., Lambert, H. and Landry, J. (2000) Inhibition of Daxx-mediated apoptosis by heat shock protein 27. Mol. Cell. Biol., 20, 7602–7612.
28. Lewis, S.E., Mannion, R.J., White, F.A., Coggeshall, R.E., Beggs, S., Costigan, M., Martin, J.L., Dillmann, W.H. and Woolf, C.J. (1999) A role for HSP27 in sensory neuron survival. J. Neurosci., 19, 8945–8953.
29. Wagstaff, M.J., Collaco-Moraes, Y., Smith, J., de Belleroche, J.S., Coffin, R.S. and Latchman, D.S. (1999) Protection of neuronal cells from apoptosis by Hsp27 delivered with a herpes simplex virus-based vector. J. Biol. Chem., 274, 5061–5069.
30. Mehlen, P., Hickey, E., Weber, L.A. and Arrigo, A.P. (1997) Large unphosphorylated aggregates as the active form of hsp27 which controls intracellular reactive oxygen species and glutathione levels and generates a protection against TNFalpha in NIH-3T3-ras cells. Biochem. Biophys. Res. Commun., 241, 187–192.
31. Rogalla, T., Ehrnsperger, M., Preville, X., Kotlyarov, A., Lutsch, G., Ducasse, C., Paul, C., Wieske, M., Arrigo, A.P., Buchner, J. and Gaestel, M. (1999) Regulation of HSP27 oligomerization, chaperone function, and protective activity agaisnt oxidative stress/tumor necrosis factor α by phospohrylation. J. Biol. Chem., 274, 18947–18956.
32. Li, S.H., Lam, S., Cheng, A.L. and Li, X.J. (2000) Intranuclear huntingtin increases the expression of caspase-1 and induces apoptosis. Hum. Mol. Genet., 9, 2859–2867.
33. Hengartner, M.O. (2000) The biochemistry of apoptosis. Nature, 407, 770–776.
34. Perez, D. and White, E. (2000) TNF-alpha signals apoptosis through a Bid-dependent conformational change in Bax that is inhibited by E1B 19K. Mol. Cell, 6, 53–63.
35. Stokoe, D., Engel, K., Campbell, D.G., Cohen, P. and Gaestel, M. (1992) Identification of MAPKAP kinase 2 as a major enzyme responsible for the phosphorylation of the small mammalian heat shock proteins. FEBS Lett., 313, 307–313.
36. Ludwig, S., Engel, K., Hoffmeyer, A., Sithanandam, G., Neufeld, B., Palm, D., Gaestel, M. and Rapp, U.R. (1996) 3pK, a novel mitogen-activated protein (MAP) kinase-activated protein kinase, is targeted by three MAP kinase pathways. Mol. Cell. Biol., 16, 6687–6697.
37. Hansen, T.O., Rehfeld, J.F. and Nielsen, F.C. (2000) Cyclic AMP-induced neuronal differentiation via activation of p38 mitogen-activated protein kinase. J. Neurochem., 75, 1870–1877.
38. Ben-Levy, R., Leighton, I.A., Doza, Y.N., Attwood, P., Morrice, N., Marshall, C.J. and Cohen, P. (1995) Identification of novel phosphorylation sites required for activation of MAPKAP kinase-2. EMBO J., 15, 4629–4642.
39. Narain, Y., Wyttenbach, A., Rankin, J., Furlong, R.A. and Rubinsztein, D.C. (1999) A molecular investigation of true dominance in Huntington's disease. J. Med. Genet., 36, 739–746.
40. Ferrari, G., Yan, C.Y. and Greene, L.A. (1995) N-acetylcysteine (D- and L-stereoisomers) prevents apoptotic death of neuronal cells. J. Neurosci., 15, 2857–2866.
41. Marsh, J.L., Walker, H., Theisen, H., Zhu, Y.Z., Fielder, T., Purcell, J. and Thompson, L.M. (2000) Expanded polyglutamine peptides alone are intrinsically cytotoxic and cause neurodegeneration in Drosophila. Hum. Mol. Genet., 9, 13–25.
42. Klement, I.A., Skinner, P.J., Kaytor, M.D., Yi, H., Hersch, S.M., Clark, H.B., Zoghbi, H.Y. and Orr, H.T. (1998) Ataxin-1 nuclear localization and aggregation: role in polyglutamine-induced disease in SCA1 transgenic mice. Cell, 95, 41–53.
43. Conway, K.A., Lee, S.J., Rochet, J.C., Ding, T.T., Williamson, R.E. and Lansbury, P.T. Jr (2000) Acceleration of oligomerization, not fibrillization, is a shared property of both alpha-synuclein mutations linked to early-onset Parkinson's disease: implications for pathogenesis and therapy. Proc. Natl Acad. Sci. USA, 97, 571–576.
44. Zhou, H., Li, S.H. and Li, X.J. (2001) Chaperone suppression of cellular toxicity of huntingtin is independent of polyglutamine aggregation. J. Biol. Chem., 276, 48417–48424.
45. Tabrizi, S.J., Workman, J., Hart, P.E., Mangiarini, L., Mahal, A., Bates, G., Cooper, J.M. and Schapira, A.H. (2000) Mitochondrial dysfunction and free radical damage in the Huntington R6/2 transgenic mouse. Ann. Neurol., 47, 80–86.
46. Polidori, M.C., Mecocci, P., Browne, S.E., Senin, U. and Beal, M.F. (1999) Oxidative damage to mitochondrial DNA in Huntington's disease parietal cortex. Neurosci. Lett., 272, 53–56.
47. Li, S.H., Cheng, A.L., Li, H. and Li, X.J. (1999) Cellular defects and altered gene expression in PC12 cells stably expressing mutant huntingtin. J. Neurosci., 19, 5159–5172.
48. Albers, D.S. and Beal, M.F. (2000) Mitochondrial dysfunction and oxidative stress in aging and neurodegenerative disease. J. Neural Transm., 59(Suppl), 133–154.
49. Preville, X., Salvemini, F., Giraud, S., Chaufour. S., Paul, C., Stepien, G., Ursini, M.V. and Arrigo, A.P. (1999) Mammalian small stress proteins protect against oxidative stress through their ability to increase glucose-6-phosphate dehydrogenase activity and by maintaining optimal cellular detoxifying machinery. Exp. Cell Res., 247, 61–78.
50. Ding, Q. and Keller, J.N. (2001) Proteasome inhibition in oxidative stress neurotoxicity: implications for heat shock proteins. J. Neurochem., 77, 1010–1017.
51. Lee MH, Hyun DH, Jenner P and Halliwell B.(2001) Effect of proteasome inhibition on cellular oxidative damage, antioxidant defences and nitric oxide production. J. Neurochem., 78, 32–41.
52. Bence, N.F., Sampat, R.M. and Kopito, R.R. (2001) Impairment of the ubiquitin–proteasome system by protein aggregation. Science, 292, 1552–1555.

53. Sawa, A., Wiegand, G.W., Cooper, J., Margolis, R.L., Sharp, A.H., Lawler, J.F. Jr, Greenamyre, J.T., Snyder, S.H. and Ross, C.A. (1999) Increased apoptosis of Huntington disease lymphoblasts associated with repeat length-dependent mitochondrial depolarization. Nature Med., 5, 1194–1198.
54. Manfredi, G. and Beal, M.F. (2000) The role of mitochondria in the pathogenesis of neurodegenerative diseases. Brain Pathol., 10, 462–472.
55. Srinivasula, S.M., Ahmad, M., Fernandez-Alnemri, T. and Alnemri, E.S. (1998) Autoactivation of procaspase-9 by Apaf-1-mediated oligomerization. Mol. Cell, 1, 949–957.
56. Mehlen, P., Kretz-Remy, C., Preville, X. and Arrigo, A.P. (1996) Drosophila hsp27 and human alphaB-crystallin expression-mediated increase in glutathione is essential for the protective activity of these proteins against TNFalpha-induced cell death. EMBO J., 15, 2695–2706.
57. Kane, D.J., Sarafian, T.A., Anton, R., Hahn, H., Gralla, E.B., Valentine, J.S., Ord, T. and Bredesen, D.E. (1993) Bcl-2 inhibition of neural death: decreased generation of reactive oxygen species. Science, 262, 1274–1277.